Molecular Vision 2014; 20:1037-1047 <http://www.molvis.org/molvis/v20/1037>
Received 29 May 2014 | Accepted 16 July 2014 | Published 19 July 2014

Genome-wide DNA methylation profiles according to *Chlamydophila psittaci* infection and the response to doxycycline treatment in ocular adnexal lymphoma

Min Joung Lee,[1,2] Byung-Joo Min,[3] Ho-Kyung Choung,[1,4] Namju Kim,[1,5] Young A Kim,[6] Sang In Khwarg[1,7]

[1]Department of Ophthalmology, College of Medicine, Seoul National University, Seoul Korea; [2]Department of Ophthalmology, Hallym University Sacred Heart Hospital, Anyang, Korea; [3]Department of Biomedical Sciences, College of Medicine, Seoul National University, Seoul, Korea; [4]Department of Ophthalmology, Seoul National University Boramae Hospital, Seoul, Korea; [5]Department of Ophthalmology, Seoul National University Bundang Hospital, Seongnam, Korea; [6]Department of Pathology, Seoul National University Boramae Hospital, Seoul, Korea; [7]Department of Ophthalmology, Seoul National University Hospital, Seoul, Korea

Purpose: To compare genome-wide DNA methylation profiles according to *Chlamydophila psittaci* (*Cp*) infection status and the response to doxycycline treatment in Korean patients with ocular adnexal extranodal marginal zone B-cell lymphoma (EMZL).

Methods: Twelve ocular adnexal EMZL cases were classified into two groups (six *Cp*-positive cases and six *Cp*-negative cases). Among the 12 cases, eight were treated with doxycycline as first-line therapy, and they were divided into two groups according to their response to the treatment (four doxy-responders and four doxy-nonresponders). The differences in the DNA methylation states of 27,578 methylation sites in 14,000 genes were evaluated using Illumina bead assay technology. We also validated the top-ranking differentially methylated genes (DMGs) with bisulfite direct sequencing or pyrosequencing.

Results: The Infinium methylation chip assay revealed 180 DMGs in the *Cp*-positive group (74 hypermethylated genes and 106 hypomethylated genes) compared to the *Cp*-negative group. Among the 180 DMGs, *DUSP22*, which had two significantly hypomethylated loci, was validated, and the correlation was significant for one CpG site (Spearman coefficient=0.6478, p=0.0262). Regarding the response to doxycycline treatment, a total of 778 DMGs were revealed (389 hypermethylated genes and 336 hypomethylated genes in the doxy-responder group). In a subsequent replication study for representative hypomethylated (*IRAK1*) and hypermethylated (*CXCL6*) genes, the correlation between the bead chip analysis and pyrosequencing was significant (Spearman coefficient=0.8961 and 0.7619, respectively, $p<0.05$).

Conclusions: Ocular adnexal EMZL showed distinct methylation patterns according to *Cp* infection and the response to doxycycline treatment in this genome-wide methylation study. Among the candidate genes, *DUSP22* has a methylation status that was likely attributable to *Cp* infection. Our data also suggest that the methylation statuses of *IRAK1* and *CXCL6* may reflect the response to doxycycline treatment.

Lymphomas of the ocular adnexa account for approximately 8% of extranodal lymphomas and are the most common malignant tumor arising from the ocular adnexa [1,2]. The incidence rose steadily between 1975 and 2001, with an annual increase of 6.3%, and geographic differences in epidemiology have been reported [3,4]. In Korea, extranodal marginal zone B-cell lymphoma of mucosa-associated lymphoid tissue (EMZL) accounts for a higher proportion (80–90%) of all ocular adnexal lymphomas than in Western countries (35–70%) [5-7]. In addition, a younger age of onset, predominance of conjunctival involvement, earlier stage of diagnosis, and better prognosis are characteristic findings in Korean patients with ocular adnexal lymphoma [5]. These geographically distinctive epidemiologic patterns suggest environmental and genetic factors, including microbiologic infection [3,4,8].

Among several microbiological agents, *Chlamydophila psittaci* (*Cp*) has been suggested as a possible etiologic agent. In 2004, Ferreri et al. reported that they detected *Cp* DNA with targeted PCR in 80% of patients with ocular adnexal EMZL [9]. However, subsequent studies revealed that the prevalence of *Cp* infection in ocular adnexal EMZL cases varied among countries [4,10,11]. Regarding South Korea, a relatively high prevalence of *Cp* positivity (75–77%) has been repeatedly reported [12,13]. In addition, *Cp*-eradicating treatment using doxycycline antibiotics has been attempted as first-line targeted therapy in South Korea [4,13,14].

Correspondence to: Sang In Khwarg, Seoul National University Hospital Ophthalmology 101 Daehak-ro, Jongno-gu, Seoul, Seoul 110-744, Republic of South Korea, Phone: 82-2-2072-2879; FAX: 82 (2) 741-3187, email: khwarg@snu.ac.kr

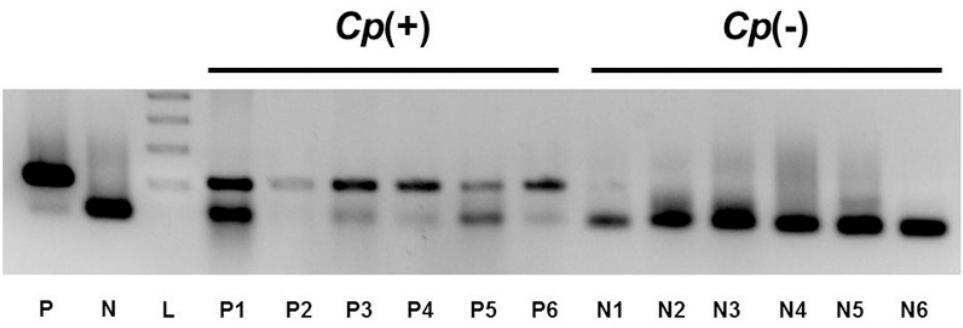

Figure 1. Amplification of *Chlamydophila psittaci* (*Cp*) DNA using PCR in ocular adnexal extranodal marginal zone B-cell lymphoma (EMZL). Six cases of 12 ocular adnexal EMZL showed positive bands and defined as *Cp*-positive samples, and the others were grouped as *Cp*-negative group. P, positive control for C. psittaci; N, negative control; L, size marker 485 (100-bp DNA ladder).

Several genetic alterations have been reported in ocular adnexal EMZLs [15]. The most common alterations are the translocations t(11;18; q21;q21), t(14;18; q32;q21), and t(1;14; p22;q32), trisomy 3 and trisomy 18. Epigenetic alterations in association with aberrant promoter hypermethylation have also been observed in mucosa-associated lymphoid tissue (MALT) lymphomas. Regarding gastric EMZL, several studies have demonstrated that *Helicobacter pylori* (*Hp*) infection is associated with gene promoter hypermethylation or hypomethylation with specific methylation profiles [16,17].

Recently, Choung et al. [13] also reported the methylation profile of nine tumor suppressor genes and reported that aberrant promoter methylation is a frequent event in ocular adnexal EMZLs. However, genome-wide screening of DNA methylation profiles associated with ocular adnexa EMZL has not been performed. In the present study, we evaluated genome-wide DNA methylation profiles associated with *Cp* infection and the response to doxycycline treatment.

METHODS

Patients: Twelve tissue samples were collected from patients who had undergone an incisional biopsy operation and had been histologically confirmed as having an EMZL at Seoul National University Hospital, Seoul National University Bundang Hospital, and Seoul National University Boramae Hospital between 2011 and 2012. In the operating room, the tumor sample was immediately divided into two pieces; one piece of tissue was sent to the pathologist for histologic examination, and the other piece was stored fresh frozen at −80 °C. The histopathologic diagnosis of the sample was confirmed by a hematopathologist.

A staging workup was performed based on a physical examination, complete ophthalmologic examination, chest radiograph, magnetic resonance imaging (MRI) of the orbit, computed tomography (CT) of the chest and abdomen, and bone marrow aspiration and biopsy. All patients were staged according to the American Joint Committee on Cancer classification [18].

All samples were examined for *Cp* positivity and divided into two groups (six *Cp*-positive samples and six *Cp*-negative samples; Figure 1). Among the 12 patients, eight patients were treated with doxycycline (100 mg twice a day for 3 weeks, two cycles) as a single, first-line treatment; they were followed for more than 6 months, and they were divided into two groups according to their treatment responses (four doxy-responders and four doxy-nonresponders). Doxycycline was given orally at a dose of 100 mg twice a day for 3 weeks, followed by 3 weeks of no doxycycline treatment, and then the treatment was repeated for an additional 3 weeks. The objective lymphoma response to the therapy was evaluated in all patients 9 weeks after the first dose, then every 3 months for 2 years, and every 6 months thereafter with biomicroscopic examination or orbital imaging study (CT or MRI) by experienced oculoplasty specialists. The response was assessed using modified international workshop criteria [19]. Complete remission (CR) was defined as the complete disappearance of all detectable ophthalmic and radiographic evidence of disease and eye-related symptoms, if they were present before therapy. Partial remission (PR) was defined as a 50% or more decrease in the sum of the product of the greatest diameters. Stable disease (SD) was defined as the regression of any measurable lesion by less than 50% or no change in size of the measurable lesions. Progressive disease (PD) was defined by the development of a new lesion or by a 50% or more increase from the smallest sum of the product of the greatest diameters. The patient demographic and clinical data are shown in Table 1. All protocols of this study adhered to the tenets of the Declaration of Helsinki and the ARVO statement on human subjects. The study was approved by the Committee on Human Research of the Seoul National University Hospital (IRB No. H-1012–086–344), and informed consent was obtained from all patients enrolled.

Table 1. Clinical characteristics of the study subjects.

Case No.	Age / Sex	Tumor location (T stage*)	*Cp*	Initial treatment	Response to treatment†	Response to Doxycycline	Follow-up-(month)
P1	64/F	Lacrimal gland (2b)	+	Doxy	CR	Yes	13
P2	39/F	Conjunctiva (1b)	+	Doxy	CR	Yes	24
P3	43/M	Orbit (2c)	+	Doxy	SD	No	17
P4	51/M	Conjunctiva (1b)	+	Doxy	PD	No	36
P5	53/F	Conjunctiva and orbit (2a)	+	Doxy	SD	No	20
P6	29/F	Conjunctiva (1b)	+	Doxy	-		4
N1	29/F	Conjunctiva (1b)	-	Doxy	CR	Yes	34
N2	49/M	Orbit (2c)	-	Doxy	SD	No	15
N3	79/F	Conjunctiva (1b)	-	Doxy	PR	Yes	15
N4	48/M	Orbit and eyelid (3)	-	RT	CR	-	4
N5	68/F	Orbit (2c)	-	-	-	-	-
N6	30/F	Conjunctiva (1b)	-	Doxy	-	-	-

* American Joint Committee on Cancer staging [18] † The response to the therapy was assessed 9 weeks after the first-dose, then every 3 months for 2 years, and then every 6 months afterward, using modified international workshop criteria [19] *Cp*, *Chlamydophila psittaci*; Doxy, doxycycline; RT, radiation therapy; CR, complete response; PD, progressive disease; PR, partial response; SD, stable disease.

Detection of Chlamydophila DNA: *Chlamydophila* DNA was generously provided by Dr. Seung-Joon Lee of Kangwon National University, Korea. The DNA was amplified with PCR and cloned using the TOPO TA cloning kit (Invitrogen, Carlsbad, CA) according to the manufacturer's instructions. For verification, the cloned DNA was sequenced in both directions with Big Dye terminator (Applied Biosystems, Foster City, CA) and analyzed using an ABI 3730XL DNA analyzer (Applied Biosystems). For each extracted DNA sample, touchdown enzyme time-release PCR (TETR-PCR) for *Cp* was performed as described previously, but with some modification of the annealing temperature. The primer sequences for *Cp* were 5'-CCC AAG GTG AGG CTG ATG AC-3' (forward) and 5'-CAA ACC GTC CTA AGA CAG TTA-3' (reverse). Ta-CLONED Chlamydophila DNA was used as a positive control. The annealing temperature was 54 °C. The amplified DNA fragments were electrophoresed on 2% agarose gels and were visualized after staining with ethidium bromide. To exclude the possibility of contamination of the extracted DNA, the PCR products positive for *Cp* DNA were sequenced.

DNA extraction and quality control: The genomic DNA was isolated using a QIAamp DNA Mini Kit (Qiagen, Hilden, Germany) according to the manufacturer's instructions. The average 260/280 ratio was 1.85. The quality of the DNA samples was checked using a NanoDrop ND-1000 UV-Vis Spectrophotometer (Thermo Fisher Scientific, Waltham, MA). Then, the samples were electrophoresed on agarose gels, and the samples with intact genomic DNA, no smearing on the agarose gel, were selected for further experiments. The intact genomic DNA was diluted to 50 ng/µl, and the quantity of the DNA was determined using a PicoGreen dsDNA quantification kit (Invitrogen).

Methylation profile: Genome-wide methylation profiling of 27,578 methylation sites in 14,000 genes was conducted with an Infinium methylation assay that combined the Illumina Infinium Whole Genome Genotyping (WGG) assay and BeadChip technology. The study included almost 13,000 genes in the NCBI CCDS database (Genome Build 36), 144 markers of methylation hotspots in cancer genes, 982 markers of cancer-related targets, and 110 miRNA promoters. One random sample from the 12 samples was hybridized to different chips (technical replicate). We obtained high reproducibility in the technical replicates ($r^2 \geq 0.98$).

Data analysis: For measuring methylation, we used the Illumina BeadStudio software to generate the level of methylation (β) value for each locus from the intensity of the methylated and unmethylated probes. The background normalization was conducted using the negative control signals from each well. Average normalization was performed to minimize the scanner-to-scanner variation; the average intensity values of the first color channel for all the wells in each chip were used to calculate the mean value, which was scaled to 1. The β was calculated as (intensity of methylated probe)/(intensity of methylated probe + intensity of unmethylated probe). Thus, β ranged between 0 (least methylated) and 1 (most methylated) and was proportional to the degree of methylated state of any particular loci. The Infinium methylation

chip data were analyzed with ArrayAssist software. To identify differentially methylated genes (DMGs) between the *Cp*-positive and *Cp*-negative samples or doxy-responder and doxy-nonresponder samples, we applied two significance criteria: (1) the p value calculated using the Student *t* test and corrected for multiple testing with the Benjamini-Hochberg adjustment and (2) the difference between the mean β values (delta mean). The genes were defined as DMGs if their *t* test p values were <0.05 and the |delta mean| (the absolute values of the delta mean) between the two groups were >0.06. The resulting differential methylation profiles were analyzed with DAVID bioinformatics resources for the Gene Set Enrichment Analysis (GSEA). A hierarchical clustering analysis was based on the Euclidean distance matrix, and the complete linkage method was performed with an R package. The color scale of the heat map represents densely methylated loci (red) to sparsely methylated loci (green).

Bisulfite direct sequencing: The targeted fragment was amplified from bisulfite-treated DNA, cloned, and sequenced to obtain an accurate map of the distribution of CpG methylation. The PCR products were then cloned into the pEasy-T1 vector (Transgen, Beijing, China), and ten colonies were randomly chosen and sequenced.

Pyrosequencing: Sodium bisulfite modification of the genomic DNA was performed. The primers were designed using the PSQ Assay Design program v.1.0.6 (Qiagen), and the sequences are presented in Table 2. The pyrosequencing was conducted using PyroMark Gold Q96 Reagents (Qiagen), and PCR was conducted using AccuPower HotStart PCR Premix (Bioneer, Daejeon, Korea). The pyrosequencing data were analyzed with Pyro Q-CpG V:1.0.9 analysis software (Qiagen).

RESULTS

Differential methylation according to Chlamydophila psittaci infection: To investigate whether ocular adnexal EMZLs have differential methylation patterns regarding *Cp* infection status, a whole-genome methylation array analysis was performed by using the Illumina Infinium Human Methylation 27 Bead Chip. When we compared all 27,578 loci, 184 CpG sites were differentially methylated at |delta mean|≥0.06 and p value <0.05. The list of differentially methylated sites is shown in Appendix 1. Four pairs of loci corresponded to the same gene; 180 genes were differentially methylated. The *Cp*-positive samples showed hypermethylation in 75 of the CpG sites (40.8%, 74 genes) and hypomethylation in 109 of the CpG sites (59.2%, 106 genes). To assess the ability of the 184 differentially methylated loci to distinguish the *Cp*-positive group from the *Cp*-negative group, the methylation patterns of the sites were hierarchically clustered by measuring the Euclidian distance between the methylation levels across the loci (Figure 2). The samples were significantly segregated according to *Cp* status.

The results of the gene set analyses using PANTHER are shown in Appendix 2. The most significant annotation clusters of enriched gene sets (p<0.05) were inferred from functional annotation analysis with DMGs according to their methylation statuses. The DMGs were enriched the most in genes for biologic processes related to immunity and defense (p=8.69E-07), followed by signal transduction (p=0.001). Regarding molecular function, DMGs were related to receptor (p=5.75E-08), ion channel (p=9.35E-05), and extracellular matrix (p=0.008).

We subsequently performed bisulfite direct sequencing for dual specificity protein phosphatase 22 *(DUSP22;* gene ID 56940), which showed the most differentially methylated loci at two sites. *DUSP22* also belongs to the gene sets of immunity and defense and signal transduction. The primers and PCR conditions are described in Table 2. The methylation state of one CpG site showed a significant correlation with

Table 2. Primer sequences for bisulfite sequencing or pyrosequencing.

Genes	Method	Sequences (5'-3')	Annealing Tm (°C)	Product size (bp)
DUSP22 (1st site)	bisulfite sequencing	F: GGGGAGTTTTTAGAGATTAGGTTTTT R: AATCTCCAAATCCCCCTTTAAC	71	131
DUSP22 (2nd site)	bisulfite sequencing	F: GTATAGAAAGTTTTGTTTTTTA R: TATTCATCCCATTCCCCATAATA	81	226
IRAK1	pyrosequencing	F: TTAAATGAGGGTTGGGGTAGTAGTAA R: ACAACAACCTTAAACCATTCAATCTC	69	109
CXCL6	pyrosequencing	F: GGTTATTGGAGAGGAGGAGTATTT R: CAACAAAATCTCATCCCCTAAACTTA	68	95

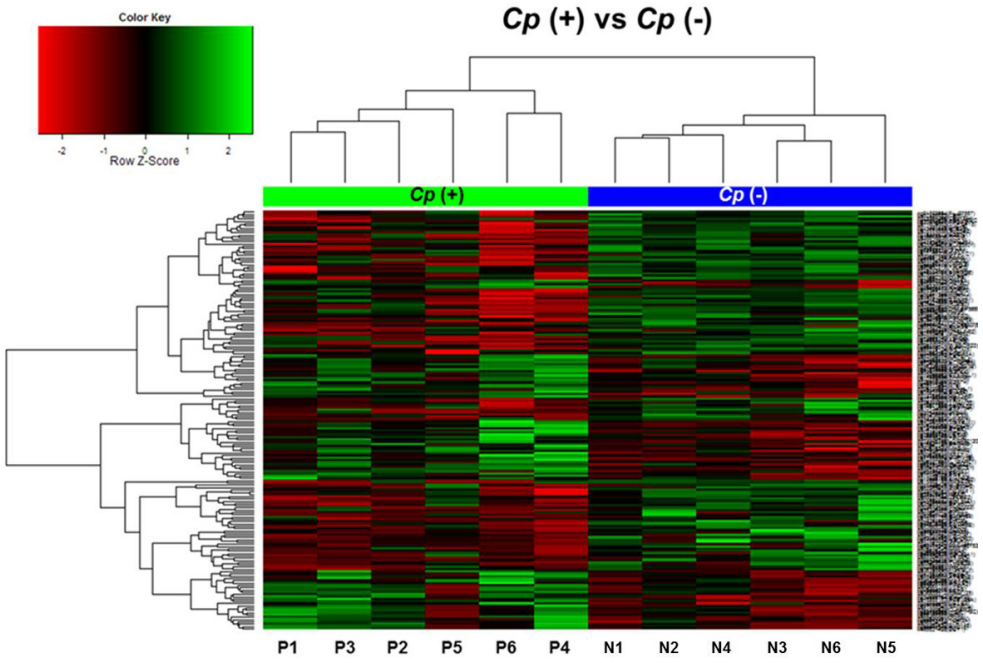

Figure 2. Hierarchical clustering analysis based on the DNA methylation data obtained from six *Chlamydophila psittaci*–positive and six *Chlamydophila psittaci*–negative ocular adnexal extranodal marginal zone B-cell lymphoma cases (*Chlamydophila psittaci* [*Cp*]-positive: P1–P6, *Cp*-negative: N1–N6). The 184 significant methylated CpG sites were selected with the criteria |delta mean| >0.06 and p<0.05. The color scale of the heat map represents densely methylated loci (red) to sparsely methylated loci (green). All cases were clearly clustered into two groups.

that of the Infinium methylation chip assay (Spearman coefficient=0.6478, p=0.0262); however, the other CpG site failed to replicate the methylation array results (Figure 3).

Differential methylation according to responsiveness to doxycycline: Regarding the doxycycline response, the general methylation level was similar between the two groups, showing a bimodal distribution. There were a total of 778 CpG sites differentially methylated at |delta mean|≥0.06 and p value<0.05. The differentially methylated CpG sites are listed in Appendix 3. Several CpG sites corresponded to the same gene, and 697 genes were differentially methylated. The doxy-responder samples showed hypermethylation in 442 of the CpG sites (56.8%, 389 genes) and hypomethylation in 336 of the CpG sites (43.2%, 308 genes). Figure 4 displays hierarchical clustering data, which clearly distinguishes the doxy-responder samples from the doxy-nonresponder samples.

The results of the gene set analyses using PANTHER are shown in Appendix 4. The most significant annotation clusters of enriched gene sets (p<0.05) were inferred from functional annotation analysis with DMGs according to their methylation statuses. The DMGs were most enriched in genes for biologic processes related to signal transduction (p=9.20E-08). Regarding molecular function, DMGs were related to the receptor (p=2.76E-08), transcription factor (p=0.00015), and extracellular matrix (p=0.00057). To validate the epigenetic control of DMGs for the response to doxycycline, we chose one hypomethylated (interleukin-1 receptor-associated kinase 1, *IRAK1;*gene ID 3654, OMIM: 300283) gene and one hypermethylated (CXC chemokine ligand 6, *CXCL6;* gene ID 6372, OMIM: 138965) gene from the signal transduction gene set.

The methylation levels of *IRAK1* and *CXCL6* were examined with pyrosequencing. The results obtained for *IRAK1* and *CXCL6* were in accordance with the results obtained by the Infinium methylation chip assay with the Spearman's rank correlation coefficient (p=0.0026, Spearman coefficient=0.8961; p=0.0368, Spearman coefficient=0.7619, respectively; Figure 5).

DISCUSSION

Using a genome-wide approach, we compared the methylation state of 27,578 loci of 14,000 genes between *Cp*-positive and *Cp*-negative samples and between samples of responders and non-responders to doxycycline treatment. The cluster analysis showed that all cases could be clearly distinguished based on their *Cp* status using 180 DMGs. The methylation profiles showed a distinct signature according to the response to doxycycline treatment with 778 DMGs.

Over the last decade, *Cp* has been proposed as a possible etiologic agent of ocular adnexal EMZL [20]. The role of *Cp* in the pathogenesis of ocular adnexal EMZL has not been fully elucidated. *Chlamydophila* species are obligate intracellular bacteria that cause persistent infections. *Cp* infection may trigger a chronic antigenic stimulus that can drive the development of acquired MALT and overt EMZLs [4]. In

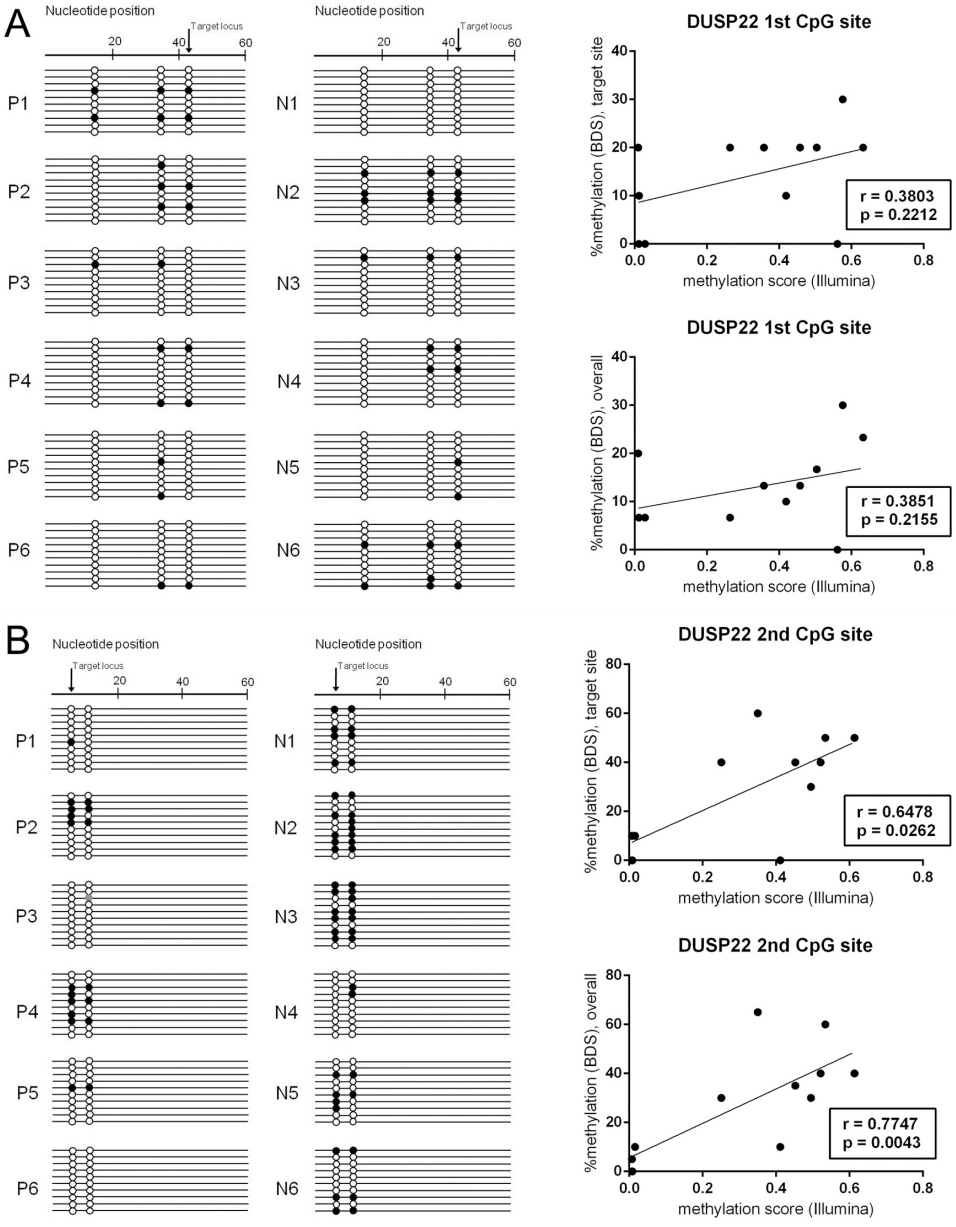

Figure 3. Results of direct bisulfite sequencing for two differentially methylated CpG sites of *DUSP22* in ocular adnexal extranodal marginal zone B-cell lymphoma. **A**: The first CpG site, target ID cg15383120, promoter, CpG island. **B**: The second CpG site, target ID cg11235426, nonpromoter, CpG island. Each row represents a bacterial clone with a circle symbolizing a CpG site. Methylated and unmethylated CpG sites are indicated by black and white circles, respectively. Mutated sites are indicated by gray circles. Correlation analysis between the Infinium methylation chip assay and bisulfite sequencing revealed that only the second CpG site showed significant correlation between the two methods.

addition to antigenic stimulation, a potential, direct oncogenic role of *Cp* has recently been suggested. Some researchers have reported that these organisms have mitogenic activity, induce oxidative damage, and cause resistance to apoptosis of the infected cells [21,22]. In this study, there were only 180 DMGs over 14,000 tested genes, and these DMGs were frequently included in gene sets of immunity and defense and signal transduction gene sets; such distinct methylation patterns are likely attributable to the *Cp* infection itself rather than different oncogenic mechanisms.

DUSP22 is an atypical *DUSP* and can activate c-Jun N-terminal kinase 1 (*JNK1;* gene ID 5599, OMIM: 601158) through the activation of the upstream mitogen-activated protein kinase kinase 3 (*MKK3;* gene ID 5606, OMIM: 602315) and *MKK7* (gene ID 5609, OMIM: 603014) [23]. *JNK*s are responsive to stress stimuli and play a role in T cell differentiation and cellular apoptosis, and dysfunctional *JNK* signaling is associated with inflammatory, vascular, neurodegenerative, metabolic, and oncological diseases. Several studies have reported the activation of the *JNK* pathway upon *Chlamydophila* infection [24,25]. In the present study, *DUSP22* was hypomethylated in the *Cp*-positive group, which may suggest that the *DUSP22* gene induces gene expression by activating transcription. In addition, *DUSP22* could act

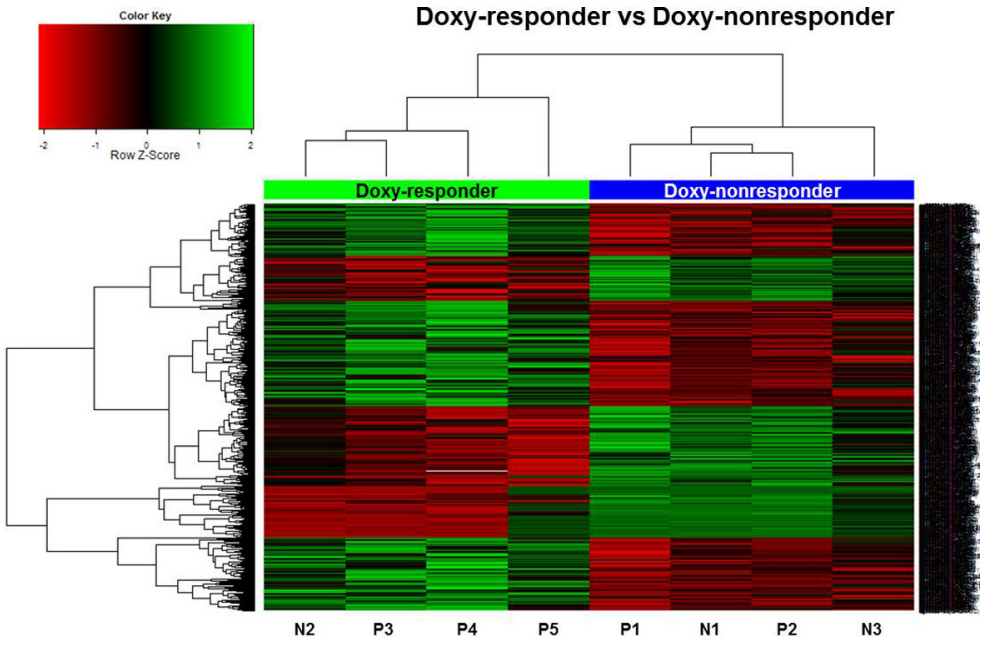

Figure 4. Cluster analysis and heatmap of methylation level between ocular adnexal extranodal marginal zone B-cell lymphoma doxy-responders (n=4) and doxy-nonresponders (n=4). The methylation levels at the 778 CpG sites were used for hierarchical clustering. All cases were clearly clustered into two groups in this dendrogram.

as a tumor suppressor gene [26]. *DUSP22* is upregulated in B-cell chronic lymphocytic leukemia in patients harboring mutations at the *IgVH* gene (ID 3509, OMIM 147070), which regarded as a good prognostic marker [27]. *DUSP22* rearrangements have recently been reported in subsets of cutaneous and systemic T-cell lymphomas [28-30]. *DUSP22* is also downregulated in breast cancers, which typically show amplification at the 8p11–12 chromosomal region [31]. *DUSP22* was recently suggested as a potential therapeutic target for these disorders [32].

The standard treatment for ocular adnexal EMZL is low-dose radiotherapy. Although radiotherapy has a high rate of local control, ranging from 80% to 100%, potential ocular toxicity and the risk of distant metastasis are major limitations. Several alternative treatment modalities are available, including chemotherapy, monoclonal anti-CD20 antibody treatment, interferon immunotherapy, and doxycycline antibiotic treatment [15]. For gastric EMZL, antibiotic therapy targeting *Helicobacter pylori* induces lymphoma regression in 6–70% of stage I_E cases [33]. Similarly, *Cp*-eradicating treatment has been suggested for ocular adnexal EMZL with an average response rate of 45% [34]. However, there is debate over the association between *Cp* status and the response to doxycycline treatment. A Korean study reported a similar response rate to doxycycline treatment regardless of *Cp* status (60% versus 60%, p=1.00) [14]. Ferreri et al. reported a better response rate in a *Cp*-positive group than in a *Cp*-negative group (64% versus 38%, p=0.25) [35]. Doxycycline treatment targets *Cp* eradication, but lymphoma regression has been observed in *Cp*-positive and *Cp*-negative patients, and other undiscovered doxycycline-sensitive organisms may be associated with ocular adnexal EMZL or that doxycycline has an antineoplastic or immunomodulatory effect [36]. Thus, we analyzed the methylation profiles according to *Cp* status and the response to doxycycline treatment separately. Only nine genes overlapped between the DMGs determined with the two criteria.

The ontologic analysis of the DMGs according to the response to doxycycline showed that methylation occurred in genes involved in various biologic processes and molecular functions. The most distinct ontologic category was signal transduction. Some genes involved in the pathogenesis of ocular adnexal EMZL deserve our attention and were validated with pyrosequencing. *IRAK1*, a serine-threonine kinase, was identified as a key component of the interleukin-1 receptor (IL-1R) signaling pathway and involved in toll-like receptor signaling [37]. *IRAK1* has recently been indicated as a gene associated with systemic lupus erythematosus. *IRAK1* also may play a regulatory role in diabetes and atherosclerosis. *CXCL6*, known as granulocyte chemotactic protein 2, is a small cytokine belonging to the chemokine family. Chemokines induce directional cellular migration during inflammation, and prolonged inflammation is thought to facilitate carcinogenesis by providing a microenvironment that is ideal for tumor cell development and growth [38]. *CXCL6* displays angiogenic effects in tumors and is upregulated in gastrointestinal tumors, lung cancer, and osteosarcoma. Interestingly, the angiogenic effect of *CXCL6* correlates with the

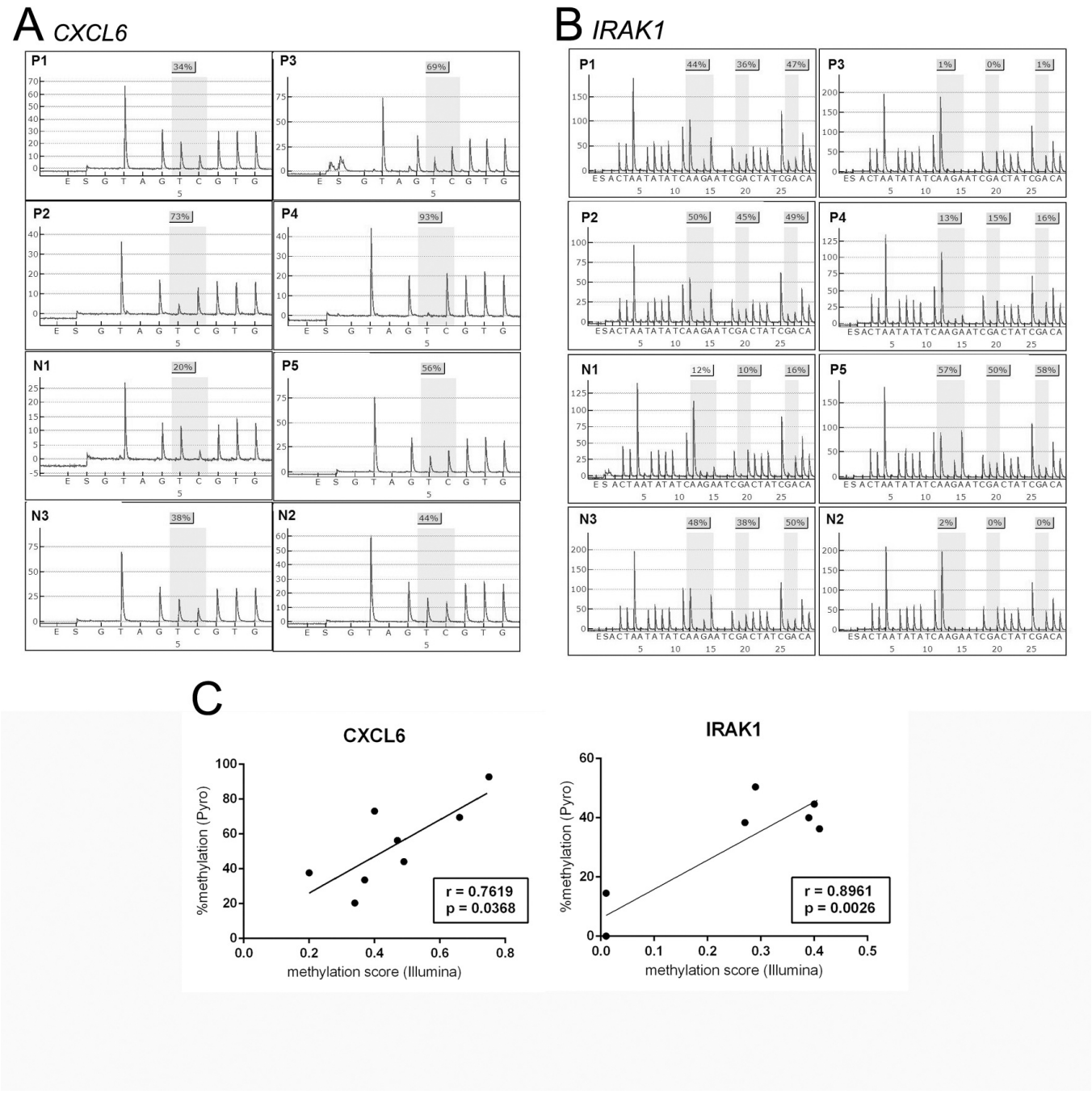

Figure 5. Validation of Infinium methylation chip assay by pyrosequencing. Pyrogram data of **A**: *CXCL6* and **B**: *IRAK1* in ocular adnexa extranodal marginal zone B-cell lymphoma. C: Correlation analysis between Infinium Methylation Chip Assay and pyrosequencing of *IRAK1* and *CXCL6*.

expression of matrix metalloproteinase (MMP)-9/gelatinase-B, and doxycycline has anti-MMP properties. In this study, the doxy-response group showed *CXCL6* hypomethylation, suggesting elevated *CXCL6* expression. This finding suggests inhibition of MMP activity is a possible mechanism of action of doxycycline in ocular adnexal EMZL, but further research is needed to clarify this point.

We used Illumina's Methylation 27 assay to evaluate DNA methylation profiles of ocular adnexal EMZL at the genome-wide level. The reproducibility of the Infinium methylation chip assay was reported to have a correlation greater than 0.98 between technical replicates [39]. In addition, the Infinium methylation chip assay has been compared to other platforms and has shown reliable results with high correlation rates ranging from 0.8 to 0.9 [40].

In this study, we used several technical approaches to validate the methylation status of the selected genes. There was a strong correlation between the pyrosequencing and array analysis when we tested *IRAK1* and *CXCL6*. For *DUSP22*, we used bisulfite direct sequencing instead of pyrosequencing to validate two differentially methylated CpG sites because the primer design for pyrosequencing was structurally problematic. For one CpG site (the second CpG site), the results were highly correlated with those of the array analysis. However, the bisulfite direct sequencing yielded a generally low level of methylation of the other CpG site (the first CpG site) of *DUSP22* in all samples, which was inconsistent with the methylation chip assay. Although bisulfite sequencing is one of the most frequently used techniques for measuring DNA methylation, the robustness of bisulfite sequencing is dependent on the number of clones examined and is subject to more cloning biases [41]. An adequate sample size and larger number of clones will be needed to overcome the variability of the results of bisulfite direct sequencing.

This study had several weaknesses. First, we analyzed four doxy-responders and four doxy-nonresponders regardless of their *Cp* status because of the small sample size. Although several studies have reported that the response rate to doxycycline treatment and *Cp* status were not associated, samples with uniform characteristics will help verify the mechanism of doxycycline treatment in ocular adnexal EMZL cases. Second, we analyzed only the DNA methylation status, and additional experiments are required explore the relationship between methylation status and mRNA expression with a much larger sample. Many epigenetic changes in cancer can be passenger events that are not pathogenic and, thus, should be supported by gene expression analysis. In future studies, the correlation between methylation status and gene expression should be addressed.

In conclusion, this study is the first report on methylation profiles based on genome-wide methylation in ocular adnexal EMZL tissues. The results demonstrated that several genes were methylated differentially regarding *Cp* infection status and the response to doxycycline treatment. Among the candidate genes, methylation of *DUSP22* was likely attributable to *Cp* infection. The methylation status of *IRAK1* and *CXCL6* differed between the doxy-responders and the doxy-nonresponders, suggesting the possible clinical application of therapies targeting those genes. Additional large-scale studies are necessary to confirm our results.

APPENDIX 1.

CpG sites differentially methylated in *Cp*-positive samples compared to *Cp*-negative samples. To access the data, click or select the words "Appendix 1."

APPENDIX 2.

CpG sites differentially methylated between Doxy-responders and Doxy-nonresponders. To access the data, click or select the words "Appendix 2."

APPENDIX 3.

Summary of gene set enrichment analysis with DMGs according to *Cp* infection. To access the data, click or select the words "Appendix 3."

APPENDIX 4.

Summary of gene set enrichment analysis with DMGs according to response to doxycycline. To access the data, click or select the words "Appendix 4."

ACKNOWLEDGMENTS

This study was supported by a grant no 03–2011–0170 from the Seoul National University Hospital Research Fund.

REFERENCES

1. Stefanovic A, Lossos IS. Extranodal marginal zone lymphoma of the ocular adnexa. Blood 2009; 114:501-10. [PMID: 19372259].

2. Coupland SE, Krause L, Delecluse HJ, Anagnostopoulos I, Foss HD, Hummel M, Bornfeld N, Lee WR, Stein H. Lymphoproliferative lesions of the ocular adnexa. Analysis of 112 cases. Ophthalmology 1998; 105:1430-41. [PMID: 9709754].

3. Moslehi R, Devesa SS, Schairer C, Fraumeni JF Jr. Rapidly increasing incidence of ocular non-hodgkin lymphoma. J Natl Cancer Inst 2006; 98:936-9. [PMID: 16818858].

4. Ferreri AJ, Dolcetti R, Du MQ, Doglioni C, Resti AG, Politi LS, De Conciliis C, Radford J, Bertoni F, Zucca E, Cavalli F, Ponzoni M. Ocular adnexal MALT lymphoma: an intriguing model for antigen-driven lymphomagenesis and microbial-targeted therapy. Ann Oncol 2008; 19:835-46. [PMID: 17986622].

5. Oh DE, Kim YD. Lymphoproliferative diseases of the ocular adnexa in Korea. Arch Ophthalmol 2007; 125:1668-73. [PMID: 18071120].

6. Yoon JS, Ma KT, Kim SJ, Kook K, Lee SY. Prognosis for patients in a Korean population with ocular adnexal lymphoproliferative lesions. Ophthal Plast Reconstr Surg 2007; 23:94-9. [PMID: 17413620].

7. Sullivan TJ, Whitehead K, Williamson R, Grimes D, Schlect D, Brown I, Dickie G. Lymphoproliferative disease of the ocular adnexa: a clinical and pathologic study with statistical analysis of 69 patients. Ophthal Plast Reconstr Surg 2005; 21:177-88. [PMID: 15942490].

8. Suarez F, Lortholary O, Hermine O, Lecuit M. Infection-associated lymphomas derived from marginal zone B cells: a model of antigen-driven lymphoproliferation. Blood 2006; 107:3034-44. [PMID: 16397126].

9. Ferreri AJ, Guidoboni M, Ponzoni M, De Conciliis C, Dell'Oro S, Fleischhauer K, Caggiari L, Lettini AA, Dal Cin E, Ieri R, Freschi M, Villa E, Boiocchi M, Dolcetti R. Evidence for an association between Chlamydia psittaci and ocular adnexal lymphomas. J Natl Cancer Inst 2004; 96:586-94. [PMID: 15100336].

10. Carugi A, Onnis A, Antonicelli G, Rossi B, Mannucci S, Luzzi A, Lazzi S, Bellan C, Tosi GM, Sayed S, De Falco G, Leoncini L. Geographic variation and environmental conditions as cofactors in Chlamydia psittaci association with ocular adnexal lymphomas: a comparison between Italian and African samples. Hematol Oncol 2010; 28:20-6. [PMID: 19728399].

11. Chanudet E, Zhou Y, Bacon CM, Wotherspoon AC, Muller-Hermelink HK, Adam P, Dong HY, de Jong D, Li Y, Wei R, Gong X, Wu Q, Ranaldi R, Goteri G, Pileri SA, Ye H, Hamoudi RA, Liu H, Radford J, Du MQ. Chlamydia psittaci is variably associated with ocular adnexal MALT lymphoma in different geographical regions. J Pathol 2006; 209:344-51. [PMID: 16583361].

12. Yoo C, Ryu MH, Huh J, Park JH, Kang HJ, Ahn HS, Lee Y, Kim MJ, Lee H, Kim TW, Chang HM, Lee JL, Kang YK. Chlamydia psittaci infection and clinicopathologic analysis of ocular adnexal lymphomas in Korea. Am J Hematol 2007; 82:821-3. [PMID: 17570512].

13. Choung HK, Kim YA, Lee MJ, Kim N, Khwarg SI. Multigene methylation analysis of ocular adnexal MALT lymphoma and their relationship to Chlamydophila psittaci infection and clinical characteristics in South Korea. Invest Ophthalmol Vis Sci 2012; 53:1928-35. [PMID: 22410569].

14. Kim TM, Kim KH, Lee MJ, Jeon YK, Lee SH, Kim DW, Kim CW, Kim IH, Khwarg SI, Heo DS. First-line therapy with doxycycline in ocular adnexal mucosa-associated lymphoid tissue lymphoma: a retrospective analysis of clinical predictors. Cancer Sci 2010; 101:1199-203. [PMID: 20345477].

15. McKelvie PA. Ocular adnexal lymphomas: a review. Adv Anat Pathol 2010; 17:251-61. [PMID: 20574170].

16. Kondo T, Oka T, Sato H, Shinnou Y, Washio K, Takano M, Morito T, Takata K, Ohara N, Ouchida M, Shimizu K, Yoshino T. Accumulation of aberrant CpG hypermethylation by Helicobacter pylori infection promotes development and progression of gastric MALT lymphoma. Int J Oncol 2009; 35:547-57. [PMID: 19639175].

17. Kaneko Y, Sakurai S, Hironaka M, Sato S, Oguni S, Sakuma Y, Sato K, Sugano K, Saito K. Distinct methylated profiles in Helicobacter pylori dependent and independent gastric MALT lymphomas. Gut 2003; 52:641-6. [PMID: 12692046].

18. Coupland SE, White VA, Rootman J, Damato B, Finger PT. A TNM-based clinical staging system of ocular adnexal lymphomas. Arch Pathol Lab Med 2009; 133:1262-7. [PMID: 19653722].

19. Cheson BD, Horning SJ, Coiffier B, Shipp MA, Fisher RI, Connors JM, Lister TA, Vose J, Grillo-Lopez A, Hagenbeek A, Cabanillas F, Klippensten D, Hiddemann W, Castellino R, Harris NL, Armitage JO, Carter W, Hoppe R, Canellos GP. Report of an international workshop to standardize response criteria for non-Hodgkin's lymphomas. NCI Sponsored International Working Group. J Clin Oncol 1999; 17:1244- [PMID: 10561185].

20. Collina F, De Chiara A, De Renzo A, De Rosa G, Botti G, Franco R. Chlamydia psittaci in ocular adnexa MALT lymphoma: a possible role in lymphomagenesis and a different geographical distribution. Infect Agent Cancer 2012; 7:8-[PMID: 22472082].

21. Sharma M, Rudel T. Apoptosis resistance in Chlamydia-infected cells: a fate worse than death? FEMS Immunol Med Microbiol 2009; 55:154-61. [PMID: 19281566].

22. Kun D, Xiang-Lin C, Ming Z, Qi L. Chlamydia inhibit host cell apoptosis by inducing Bag-1 via the MAPK/ERK survival pathway. Apoptosis 2013; 18:1083-92. [PMID: 23708800].

23. Shen Y, Luche R, Wei B, Gordon ML, Diltz CD, Tonks NK. Activation of the Jnk signaling pathway by a dual-specificity phosphatase, JSP-1. Proc Natl Acad Sci USA 2001; 98:13613-8. [PMID: 11717427].

24. Rodriguez N, Lang R, Wantia N, Cirl C, Ertl T, Durr S, Wagner H, Miethke T. Induction of iNOS by Chlamydophila pneumoniae requires MyD88-dependent activation of JNK. J Leukoc Biol 2008; 84:1585-93. [PMID: 18799752].

25. Krüll M, Kramp J, Petrov T, Klucken AC, Hocke AC, Walter C, Schmeck B, Seybold J, Maass M, Ludwig S, Kuipers JG, Suttorp N, Hippenstiel S. Differences in cell activation by Chlamydophila pneumoniae and Chlamydia trachomatis infection in human endothelial cells. Infect Immun 2004; 72:6615-21. [PMID: 15501794].

26. Nunes-Xavier C, Roma-Mateo C, Rios P, Tarrega C, Cejudo-Marin R, Tabernero L, Pulido R. Dual-specificity MAP kinase phosphatases as targets of cancer treatment.

Anticancer Agents Med Chem 2011; 11:109-32. [PMID: 21288197].

27. Jantus Lewintre E, Reinoso Martin C, Garcia Ballesteros C, Pendas J, Benet Campos C, Mayans Ferrer JR, Garcia-Conde J. BCL6: somatic mutations and expression in early-stage chronic lymphocytic leukemia. Leuk Lymphoma 2009; 50:773-80. [PMID: 19367498].

28. Bisig B, Gaulard P, de Leval L. New biomarkers in T-cell lymphomas. Best Pract Res Clin Haematol 2012; 25:13-28. [PMID: 22409820].

29. Karai LJ, Kadin ME, Hsi ED, Sluzevich JC, Ketterling RP, Knudson RA, Feldman AL. Chromosomal rearrangements of 6p25.3 define a new subtype of lymphomatoid papulosis. Am J Surg Pathol 2013; 37:1173-81. [PMID: 23648461].

30. Sciallis AP, Law ME, Inwards DJ, McClure RF, Macon WR, Kurtin PJ, Dogan A, Feldman AL. Mucosal CD30-positive T-cell lymphoproliferations of the head and neck show a clinicopathologic spectrum similar to cutaneous CD30-positive T-cell lymphoproliferative disorders. Mod Pathol 2012; 25:983-92. [PMID: 22388754].

31. Bernard-Pierrot I, Gruel N, Stransky N, Vincent-Salomon A, Reyal F, Raynal V, Vallot C, Pierron G, Radvanyi F, Delattre O. Characterization of the recurrent 8p11–12 amplicon identifies PPAPDC1B, a phosphatase protein, as a new therapeutic target in breast cancer. Cancer Res 2008; 68:7165-75. [PMID: 18757432].

32. Patterson KI, Brummer T, O'Brien PM, Daly RJ. Dual-specificity phosphatases: critical regulators with diverse cellular targets. Biochem J 2009; 418:475-89. [PMID: 19228121].

33. Isaacson PG, Du MQ. MALT lymphoma: from morphology to molecules. Nat Rev Cancer 2004; 4:644-53. [PMID: 15286744].

34. Kiesewetter B, Raderer M. Antibiotic therapy in nongastrointestinal MALT lymphoma: a review of the literature. Blood 2013; 122:1350-7. [PMID: 23770778].

35. Ferreri AJ, Ponzoni M, Guidoboni M, Resti AG, Politi LS, Cortelazzo S, Demeter J, Zallio F, Palmas A, Muti G, Dognini GP, Pasini E, Lettini AA, Sacchetti F, De Conciliis C, Doglioni C, Dolcetti R. Bacteria-eradicating therapy with doxycycline in ocular adnexal MALT lymphoma: a multicenter prospective trial. J Natl Cancer Inst 2006; 98:1375-82. [PMID: 17018784].

36. Ferreri AJ. Activity of clarithromycin in mucosa-associated lymphoid tissue-type lymphomas: antiproliferative drug or simple antibiotic? Chest 2011; 139:724-5. , author reply 5–6.. [PMID: 21362665].

37. Gottipati S, Rao NL, Fung-Leung WP. IRAK1: a critical signaling mediator of innate immunity. Cell Signal 2008; 20:269-76. [PMID: 17890055].

38. Vandercappellen J, Van Damme J, Struyf S. The role of CXC chemokines and their receptors in cancer. Cancer Lett 2008; 267:226-44. [PMID: 18579287].

39. Bibikova M, Le J, Barnes B, Saedinia-Melnyk S, Zhou L, Shen R, Gunderson KL. Genome-wide DNA methylation profiling using Infinium(R) assay. Epigenomics 2009; 1:177-200. [PMID: 22122642].

40. Bock C, Tomazou EM, Brinkman AB, Muller F, Simmer F, Gu H, Jager N, Gnirke A, Stunnenberg HG, Meissner A. Quantitative comparison of genome-wide DNA methylation mapping technologies. Nat Biotechnol 2010; 28:1106-14. [PMID: 20852634].

41. Reed K, Poulin ML, Yan L, Parissenti AM. Comparison of bisulfite sequencing PCR with pyrosequencing for measuring differences in DNA methylation. Anal Biochem 2010; 397:96-106. [PMID: 19835834].

Articles are provided courtesy of Emory University and the Zhongshan Ophthalmic Center, Sun Yat-sen University, P.R. China. The print version of this article was created on 19 July 2014. This reflects all typographical corrections and errata to the article through that date. Details of any changes may be found in the online version of the article.